数理解析研究所講究録
602 巻 1986 年 100-115

Hopf bifurcation of a Constrained Circuit

徳永 隆治 (Ryuji Tokunaga)

Department of Electrical Engineering
Waseda University, Tokyo, 160, Japan

ABSTRACT

A repelling torus has been observed in an extremly simple electrical circuit. The paper explains the mechanism of how the repelling torus is born in terms of "Hopf bifurcation" of a constrained system in the sense of Ikegami[5].

I. INTRODUCTION

Consider the circuit of Fig.1(a) where the non-linear resistor is characterized by Fig.1(b) and where the capacitance on the right hand side has a negative value $-C_1$. The dynamics of the circuit is governed by the state equation

$$\begin{aligned} C_1\frac{dVc_1}{dt} &= -g(Vc_2 - Vc_1) \\ C_2\frac{dVc_2}{dt} &= -g(Vc_2 - Vc_1) - i_L \\ L\frac{di_L}{dt} &= Vc_2 \end{aligned} \qquad (1)$$

where Vc_1, Vc_2 and i_L denote the voltage across C_1, the voltage across C_2 and the current through L, respectively. The function $g(\cdot)$ denotes the v-i characteristic of the non-linear resister and is described by

$$g(V) = -m_0 V + 0.5(m_0 + m_1)[\,|V + E_1| - |V - E_1|\,]. \qquad (2)$$

Note that this is the only one non-linear element in the circuit.

/

To simplify our analysis, let us transform (1) to the following dimension less form:

$$\begin{aligned} \frac{dX}{dt} &= -\alpha\, f(Y-X) \\ \frac{dY}{dt} &= -f(Y-X) - Z \\ \frac{dZ}{dt} &= \beta Y \end{aligned} \qquad (3)$$

where

$$X = Vc_1/E_1,\ Y = Vc_2/E_1,\ Z = i_L/E_1C_2,$$

$$\alpha = C_2/C_1,\ \beta = 1/LC_2,\quad a = m_0/C_2,\quad b = m_1/C_2, \qquad (4)$$

$$f(X) = -aX + 0.5\,(a+b)\,[\,|X+E_1| - |X-E_1|\,]. \qquad (5)$$

The dynamics associated with (3) depends on four parameters: a, b, α and β. In this paper we will choose α and β as our bifurcation parameters by fixing the other parameters as follows:

$$a = 0.07,\ b = 0.1. \qquad (6)$$

Figure 2 shows the bifurcation diagram in the (α,β)-parameter space. One of the most interesting featurs of (3) is that a 2-dimensional torus [1] is observed for a large range of parameter values, as well as phase locked states[2]. The number **n : m** indicates an n : m phase-locking. **C** denotes region where chaos is observed, while **DS** denotes the region where the double scroll attractor[3] is observed. **DIV** indicates the line $\alpha = 1$ where the divergence of (3) is zero. Now, a typical 1-parameter bifurcations, e.g., $\beta = 1$ looks like the following: for $\alpha < 1$, a repelling torus* is observed while there is an attractive periodic orbit inside it (see Fig.3(a)). For $\alpha > 1$, an attractive torus is observed while there is a repelling periodic orbit inside (see Fig.3(b)). Further increase of a gives rise to phase-locking as well as 2-dimensional torus, alternately many times, and finally a chaos. The chaos appears to be a folded torus chaos.[1]

* Note that equation (3) is symmetric with respect to the origin, hence there is a twin torus located symmetrically with respect to the origin. Figure 3 shows only one of them in the half space $X > 0$.

If one increases a further, the two chaotic attractors (recall that the (3) is symmetric with respect to the origin) collide with each other and becomes the double scroll.[2] Finally the double scroll dies when a boundary crisis [4] happens. If we consider an appropriate Poincaré map in the state space, we see that the periodic point (for $\alpha < 1$), bifurcates into a circle (for $\alpha > 1$). This means that a Hopf bifurcation for the Poincaré map takes place at $\alpha = 1$. A question arises then:

How is the attractive periodic orbit ($\alpha < 1$) born ?

A natural first guess would be a Hopf bifurcation at $\alpha = 0$ for the flow. It turns out that this is not the case. In order to explain this let us look at the equilibria of (3) (see Fig.4):

$$\mathbf{0} = (0,0,0),\ \mathbf{P^+} = (1+ b/a,0,0)\ ,\ \mathbf{P^-} = (-1-b/a,0,0). \qquad (7)$$

By the Routh's method one sees that the equilibrium **0** is a sink (stable) if and only if $a < 0$. On the other hand, the equilibrium $\mathbf{P^+}$ is a source (unstable) if and only if $a < 0$. Therefore there is neither non-trivial attractor nor non-trivial repellor when $\alpha < 0$. The characteristic equation at **0** (resp. $\mathbf{P^+}$) is described by

$$\lambda^3 + (1-\alpha)b\lambda^2 + \beta\lambda - \alpha\beta b \quad (\text{resp. } \lambda^3 - (1-\alpha)a\lambda^2 + \beta\lambda + \alpha\beta a\ ). \qquad (8)$$

Within the range of our parameter values the eigen values at **0** (resp. $\mathbf{P^+}$) always consist of one real γ_0 (resp. γ_p) and a complex conjugate pair $\sigma_o \pm j\omega_o$ (resp. $\sigma_p \pm j\omega_p$). Therefore, the following holds:

$$\alpha\beta b = \gamma_0(\sigma_o^2 + \omega_o^2) \quad (\text{resp. } \alpha\beta a = -\gamma_p(\sigma_p^2 + \omega_p^2)\ ). \qquad (9)$$

and hence

$$\text{if } \alpha < 0, \text{ then } \gamma_0 < 0 \ (\text{resp. } \gamma_p > 0)$$
$$\text{if } \alpha > 0, \text{ then } \gamma_0 > 0 \ (\text{resp. } \gamma_p < 0). \qquad (10)$$

Recall that **0** is a sink for $a < 0$ and P^+ is a source for $\alpha < 0$. Equation (10) tells us that only the real eigen value γ_0 (resp. γ_p) changes its sign at **0** (resp. P^+) and hence it is not a Hopf bifurcation. Then the following new question arises:

What happens to the replling torus as $\alpha \to 0$?

The objective of this paper is to report how the repelling torus and periodic attractor are born from the view point of constrained systems.[5] In the next section, we transform equation (3) into a constrained equation and we will point out the relationship between "Hopf bifurcation" of the constrained system and the appearence of the repelling torus and periodic attractor.

II. Constrained Circuit

2.1 The Dynamics

In order to answer the question in the previous section, we will change the time scale by

$$\varepsilon = \alpha, \quad \tau = \varepsilon t. \tag{11}$$

and transform (3) into the following:

$$\begin{aligned} \varepsilon \frac{di}{dt} &= \beta V \\ \varepsilon \frac{dV}{dt} &= -f(V-\mu) - i \\ \frac{d\mu}{dt} &= -f(V-\mu) \end{aligned} \tag{12}$$

where we changed the symbols of the state variables X,Y,Z into i,v and μ, respectively. For ε very small, the first two equation dominate the last equation and describe the "fast" motion while the last equation describes the "slow" motion.

Therefore, the variable μ behaves like it is almost "frozen" compared with the motion of i and v. Such a system is called a constrained system[5]. In order to study the behavior of (12) with ε very small, it is convenient to consider the plane L_μ (μ = constant) which is parallel to the (i,v)-plane. The plane L_μ is a "state space" when μ is "frozen" and is called a leaf.

Consider the "frozen fixed point" $^*P_\mu$ on L_μ :

$$P_\mu = (f(\mu),0). \tag{13}$$

Let us partition the i-v-μ state space into 3 parallel regions R^+,R^0 and R^- separated by boundaries B_{1+} and B_{1-}, respectively, where

$$\begin{aligned} R^+ &= \{ (i,v,\mu) \mid v-\mu < -1 \} \\ R^0 &= \{ (i,v,\mu) \mid |v-\mu| < 1 \} \\ R^- &= \{ (i,v,\mu) \mid v-\mu > 1 \} \\ B_{1+} &= \{ (i,v,\mu) \mid v-\mu = -1 \} \\ B_{1-} &= \{ (i,v,\mu) \mid v-\mu = 1 \}. \end{aligned} \tag{14}$$

The frozen dynamics is given by

$$\varepsilon \frac{di}{dt} = \beta V \ , \quad \varepsilon \frac{dV}{dt} = -i - b(V-\mu) \quad , \ (i,V,\mu) \in L_\mu \cap R^0, \tag{15}$$

$$\varepsilon \frac{di}{dt} = \beta V \ , \quad \varepsilon \frac{dV}{dt} = -i + a(V-\mu+\mu_+), \ (i,V,\mu) \in L_\mu \cap R^+, \tag{16}$$

where $\mu_+ = 1+b/a$. In the following, we will consider artifical dynamics (15) and (16) by freezing a value of μ. It follows from (13) and (15) that the frozen fixed point P_μ lies in $L_\mu \cap R^0$ for $0 \le |\mu| < 1$ and is stable focus and that P_μ lies in $L_\mu \cap R^+$ for $1 < \mu$ (resp. in $L_\mu \cap R^-$ for $-1 > \mu$) and is unstable focus.

* This is not a real fixed point of (12). Rather, it is a fixed point when μ is fixed.

At $\mu = 1$, however, P_1 (resp. P_{-1}) lies on the boundary $L_1 \cap B_{1+}$ (resp. $L_{-1} \cap B_{1-}$) (see Fig.5(a)). Let $\Psi^\tau(x)$ be the "frozen flow" on L_1 which is generated by (15) and which starts from an initial condition x with forward time: $\tau > 0$. Let $\Phi^{\tau'}(x)$ be the "frozen flow" on L_1 which is generated by (16) and which starts from an initial condition x with backward time: $\tau' < 0$. Pick an initial condition on the following set:

$$x_0 = \{ (i,v,\mu) \mid i < f(1) , \ v = 0 \}. \qquad (17)$$

While the frozen flow $\Psi^\tau(x)$ is rotating counter-clockwise around P_1, the frozen flow $\Phi^{\tau'}(x)$ is rotating clockwise. Let x_1 and x_2 be the points where $\Psi^\tau(x_0)$ and $\Phi^{\tau'}(x_0)$ hit $L_1 \cap B_{1+}$ for the first time (see Fig.5(b)). Note that

$$\begin{aligned} &\text{if } a > b \text{ then } | x_2 - f(1) | < | x_1 - f(1) | \\ &\text{if } a = b \text{ then } | x_2 - f(1) | = | x_1 - f(1) | \\ &\text{if } a < b \text{ then } | x_2 - f(1) | > | x_1 - f(1) | \end{aligned} \qquad (18)$$

Hence, the frozen fixed point P_1 is a centre if a = b, and is a stable focus (resp. unstable focus) if b > a (resp. b < a). It follows from (6) that P_1 is a stable focus in the present parameter values.

2.2 Bifurcations of a Second Order Circuit

Consider the simple second order autonomous circucit of Fig.6 whose dynamics is described by

$$\begin{aligned} \frac{\varepsilon}{\beta} \frac{di}{dt} &= V \\ \varepsilon \frac{dV}{dt} &= -f(V-\mu) - i \end{aligned} \qquad (19)$$

where μ,v and i denote the voltage across the DC-voltage source, the voltage across the capacitor and the current through the inductor. Function f(·) is the v-i characteristic of the non-linear resistor and is similar to (5). Note that this circuit is a van der Pol oscillator if DC-voltage source is shorted, i.e., $\mu = 0$ and if the active part and pasive part of f(·) exchange their roles. Equation (12) tells us that 2-dimensional state space of this circuit is associated with L_μ. Taking μ as the bifurcation parameter, and fixing $\beta = 1$, let us study the one parameter bifurcation of (19). At $\mu = 0$, unstable limit cycle C_0^u exists, because of the v-i caharacteristic of the non-linear resistor. As $|\mu|$ increases, the operating point of the non-linear resistor moves from the origin toward the break point. For $0 < |\mu| < 1$, unstable limite cycle C_μ^u is observed. Across $|\mu| = 1$, the operating point enters into the active part, hence the stable limite cycle C_μ^s appears from P_1 via a Hopf bifurcation. It is interesting to see that C_μ^u co-exists with C_μ^s for $1 < |\mu| < \mu^*$ (≈ 1.33). At $|\mu| = \mu^*$, C_μ^u collides with C_μ^s and becomes a semi-stable* periodic orbit C_{μ^*}. Finally, for $|\mu| > \mu^*$, both of them disappear via a saddle-node bifurcation (see Fig.7).

2.3 Appearence of the repelling torus and the periodic attractor

With the help of the observations of **2.2**, we will explain how the repelling torus and the periodic attractor are born. Define

$$\Sigma^u = \bigcup_{\mu>0}^{\mu=\mu^*} C_\mu^u \quad , \quad \Sigma^s = \bigcup_{\mu>1}^{\mu=\mu^*} C_\mu^s$$
$$F^u = \bigcup_{\mu>0}^{\mu=1} P_\mu^u \quad , \quad F^s = \bigcup_{\mu>1} P_\mu^s \qquad (21)$$

where the superscripts **s** and **u** stand for stable and unstable periodic orbits or frozen fixed points, respectively . Figure 8 shows the relative positions of these sets in the state space. Figure 9(a) shows the trajectory by solving the constrained equation (12) with $\beta = 1$ and $\varepsilon = 0.001$. Periodic orbit of Fig.9(a) is observed with forward time, and the object surrounding the periodic orbit is observed with backward time.

* If we pick an intial condition inside of this periodic orbit, the flow with forward time converges to it, on the other hand, if we pick an initial condition outside of this periodic orbit, the flow with backward time converges to it.

Now we illustrate the typical behavior of the flow in order to associate the repelling torus with the repelling object of Fig.9. Let $\Psi^{\tau}(x_0)$ be the flow generated by (12) starting from an initial condition x_0. Pick x_0 in a neighborhood of P_0,i.e.,**0**. Then $\Psi^{\tau}(x_0)$ is attracted to F^s with rapid rotation around F^s and moves up very slowly staying very close to F^s. After $\Psi^{\tau}(x_0)$ reaches a point very close to the frozen fixed point P_1, P_μ becomes unstable and $\Psi^{\tau}(x_0)$ is constrained onto Σ^s,and further moves upward with rapid rotation around F^u. Finally $\Psi^{\tau}(x_0)$ stops moving up before reaching L_{μ^*},i.e., $\Psi^{\tau}(x_0)$ converges to the periodic attractor. Note that this periodic attractor appears via a "Hopf bifurcation" at L_1 in the sense described in [5]. On the other hand, if one picks an initial condition x_1 on L_μ ($1 < \mu < \mu^*$), then $\Psi^{\tau}(x_1)$ is attracted to Σ^s with rapid rotation and moves downward very slowly staying very close to Σ^s. And finally $\Psi^{\tau}(x_1)$ converges to the periodic attractor. Now we turn to discuss the appearence of the repelling object. Let $\Phi^{\tau'}(x)$ be the flow generated by (12) starting from an initial condition x with backward time: $\tau' < 0$. Pick an initial condition x_2 in a neighborhood of $P_{\mu+}$, i.e., P^+. $\Phi^{\tau'}(x_2)$ is attracted to F^u with rapid rotation and moves downward very slowly staying very close to F^u. As soon as $\Phi^{\tau'}(x_2)$ hits a point very close to the frozen stable fixed point P_1, $\Phi^{\tau'}(x_2)$ is attracted to Σ^u and starts moving upward on Σ^u with rapid rotation. After $\Phi^{\tau'}(x_2)$ reaches L_{μ^*}, $\Phi^{\tau'}(x_2)$ is attracted to F^u again, because of disappearence of Σ^u and Σ^s. Next, pick an initial condition x_3 in a neighborhood of P_0,i.e.,**0**. Then $\Phi^{\tau'}(x_3)$ converges to Σ^u with rapid rotation and moves upward very slowly staying very close to Σ^u, and finally $\Phi^{\tau'}(x_3)$ is attracted to F^u. If this process is repeated many times, then a repelling object will be observed. Note that the repelling object of Fig.9(a) is a "holeless" torus. If ε is increased by an appropriate amount, the attraction toward F^u and Σ^u is weakened and a "hole" of the torus is discernible.

ACKNOWLEDGEMENT

The auther would like to thank T.Matsumoto of Waseda University, G.Ikegami of Nagoya University, M.Komuro of Numazu College of Technology, H.Kokubu of Kyoto University for useful discussions.

REFERENCES

[1] R.Tokunaga, "Torus-breakdown in a third-order autonomous circuit", Singakugihou, Vol.85, No.230, CAS, 1985, PP. 25-32.

[2] L.Glass and R.Perez, "Fine Structure Phase Locking", Physical Review Letters, Vol.48, No.26,1982, PP.1772-1775.

[3] T.Matsumoto, L.O.Chua and M.Komuro, "The Double Scroll", IEEE Trans, Circuits and System. CAS -32, August, 1985, PP.797-818.

[4] T.Matsumoto, L.O.Chua and M.Komuro, "The Double Scroll Bifurcations", Circuit Theory and Applications, Vol.14, 1986, PP.117-146.

[5] G.Ikegami, "Singular perturbations for constraint system" , Nagoya University, Department of Mathematics, College of General Education preprint series, 1985.

FIGURE CAPTION

Figure 1 (a) A simple electrical circuit with attracting and repelling tori.
(b) The v-i characteristic of the non-linear resistor.

Figure 2 Bifurcation diagram in the (a,b)-parameter space.

Figure 3 (a) Attracting torus and periodic repeller at a = 2 and b = 1.
(b) Repelling torus and periodic attractor at a = 0.5 and b = 1.

Figure 4 The relative positions of the equilibria and torus.

Figure 5 (a) The relative positions of L_μ and the boundaries.
(b) The flow on L_1.

Figure 6 A second order circuit.

Figure 7 Family of periodic orbits in the (i,V)-state space.

Figure 8 The relative positions of subsets in the state space.

Figure 9 Trajectory at $\beta = 1$ and $\varepsilon = 0.001$.

Figure 10 Typical trajectories in the (i,V,μ)-state space.
(a) A typical trajectory in foward time.
(b) A typical trajectory in backward time.

Figure 1

(a)

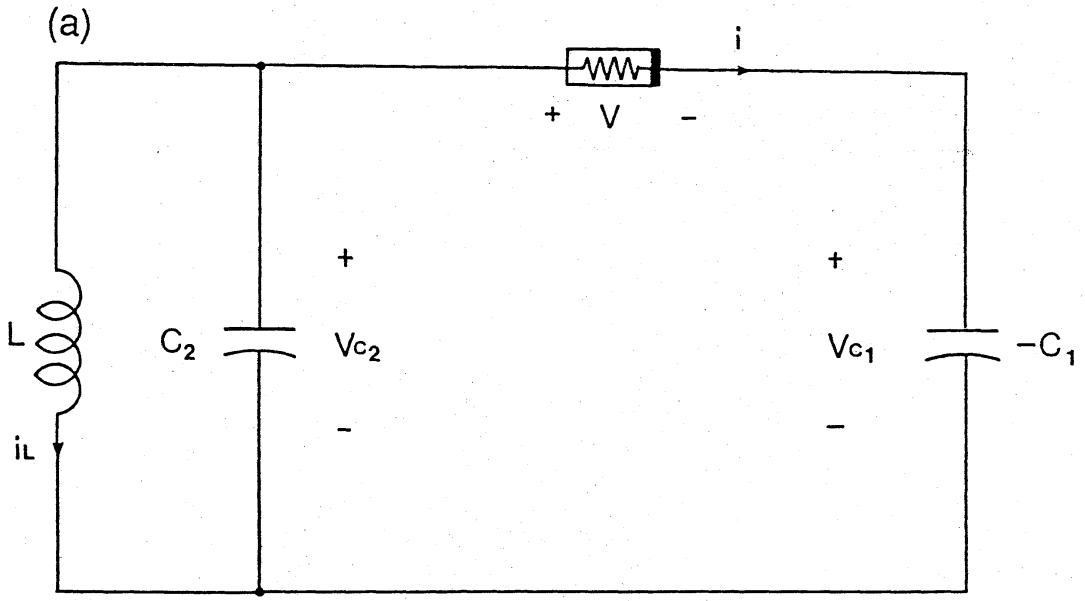

(b)

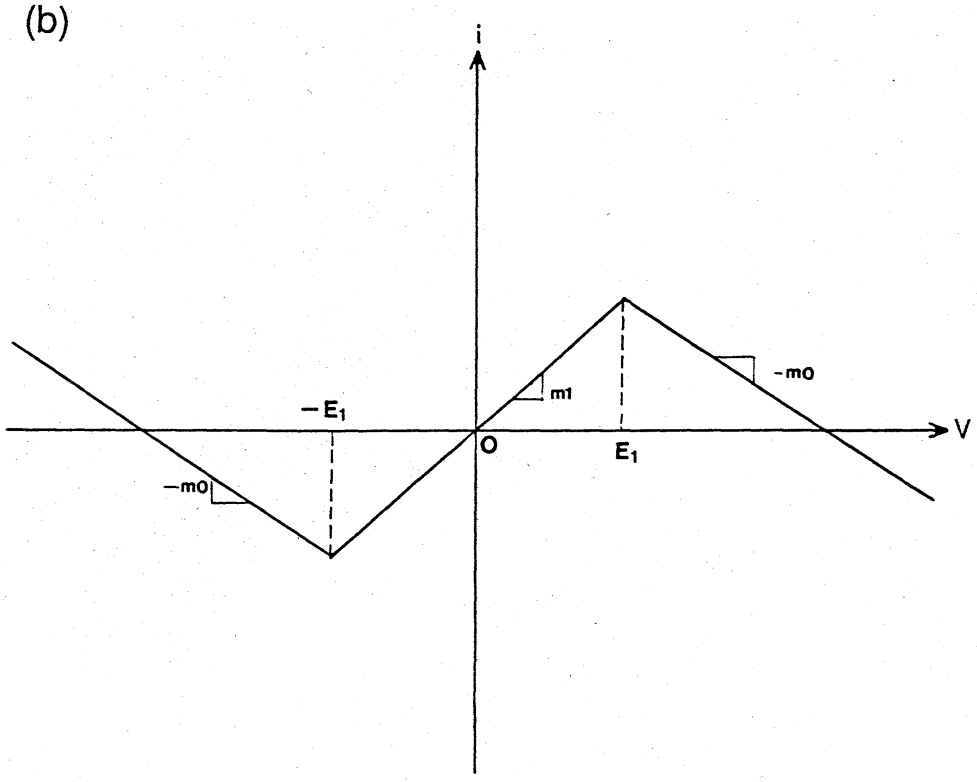

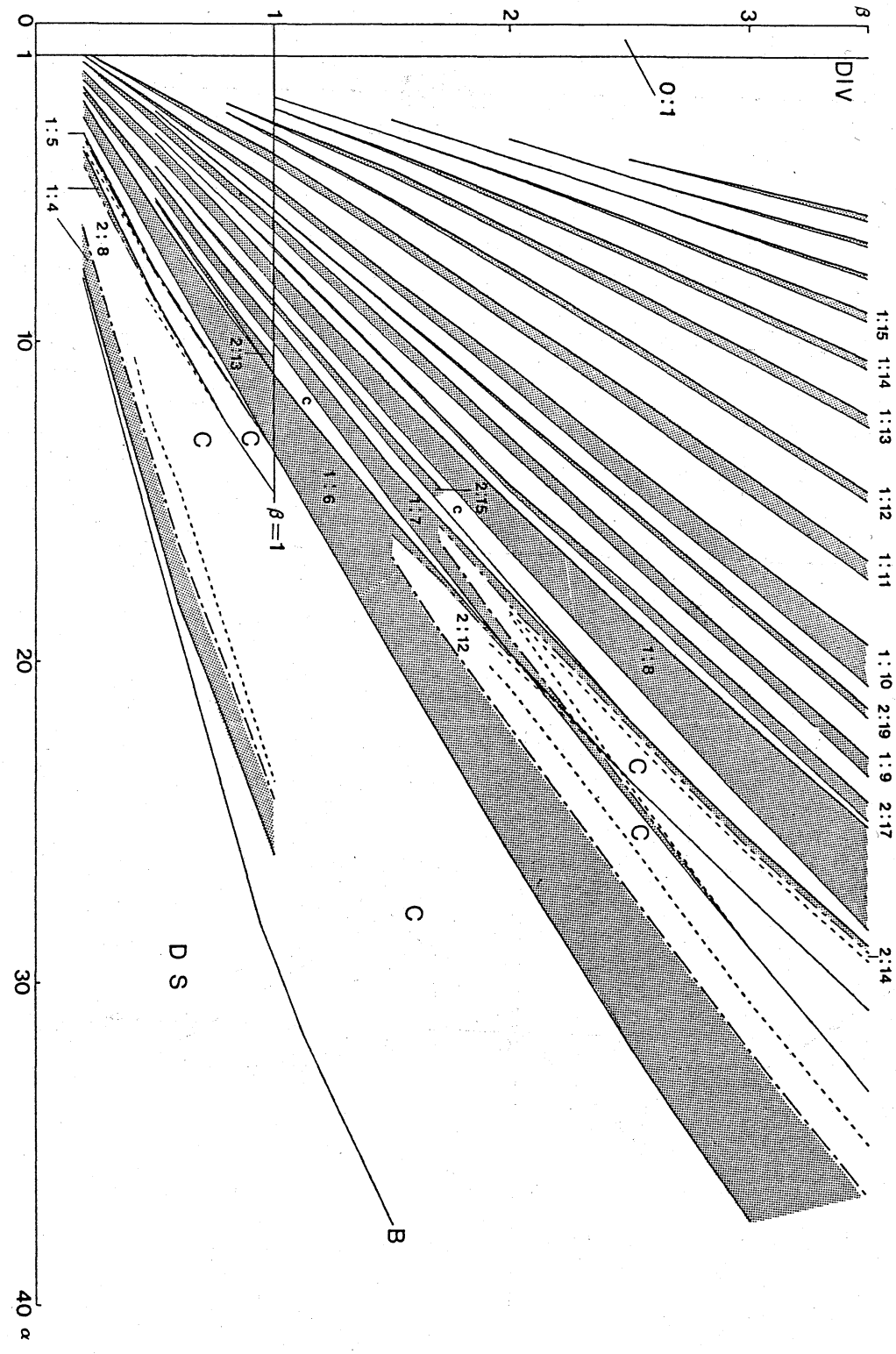
β
DIV
0:1
1:15
1:14
1:13
1:12
1:11
1:10
2:19
1:9
2:17
2:14
1:8
2:15
2:12
1:7
1:6
2:13
2:8
1:5
1:4
β=1
C
C
C
C
C
C
C
D S
B
0
1
10
20
30
40
α

Figure 2

Figure 3

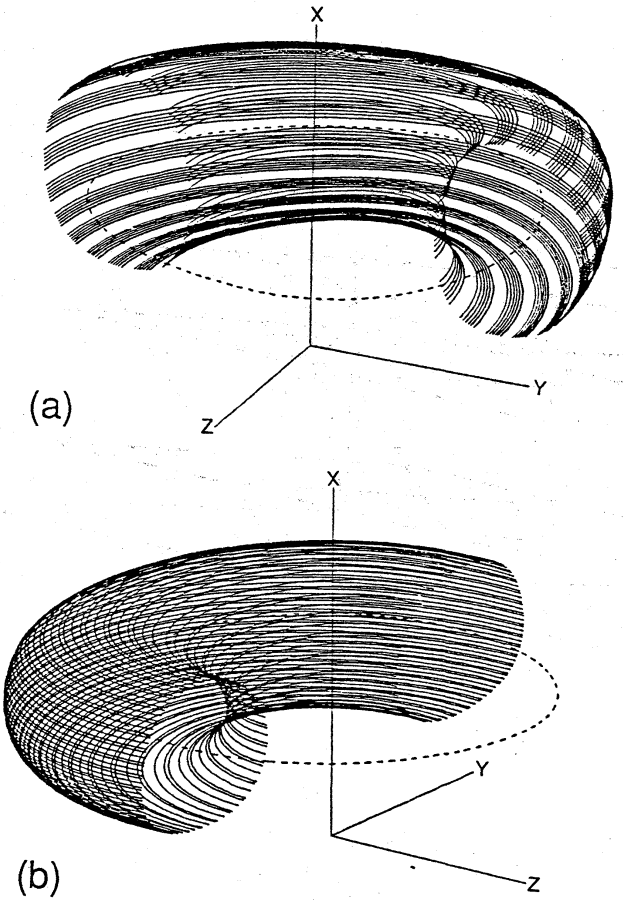

Figure 4

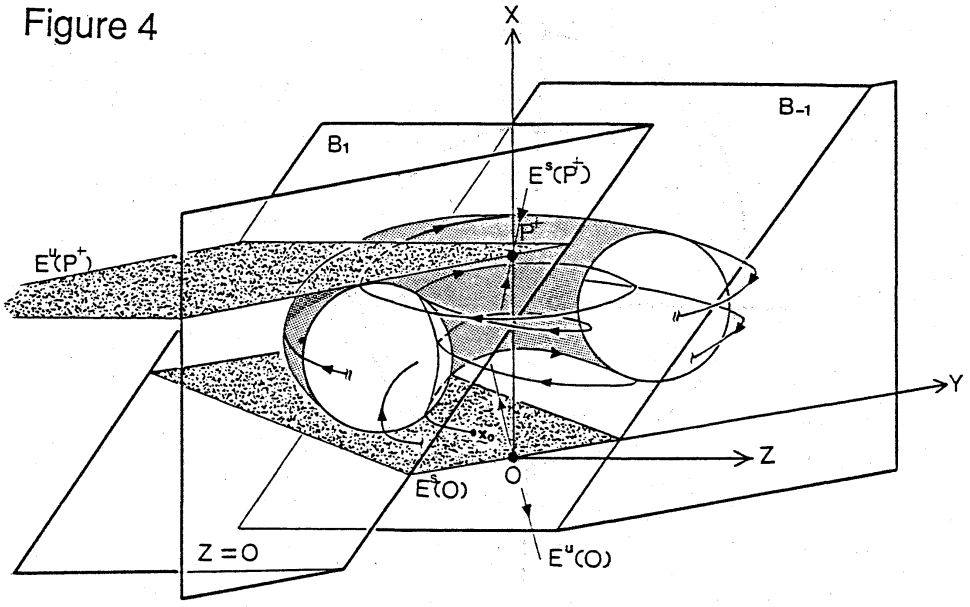

Figure 5

(a)

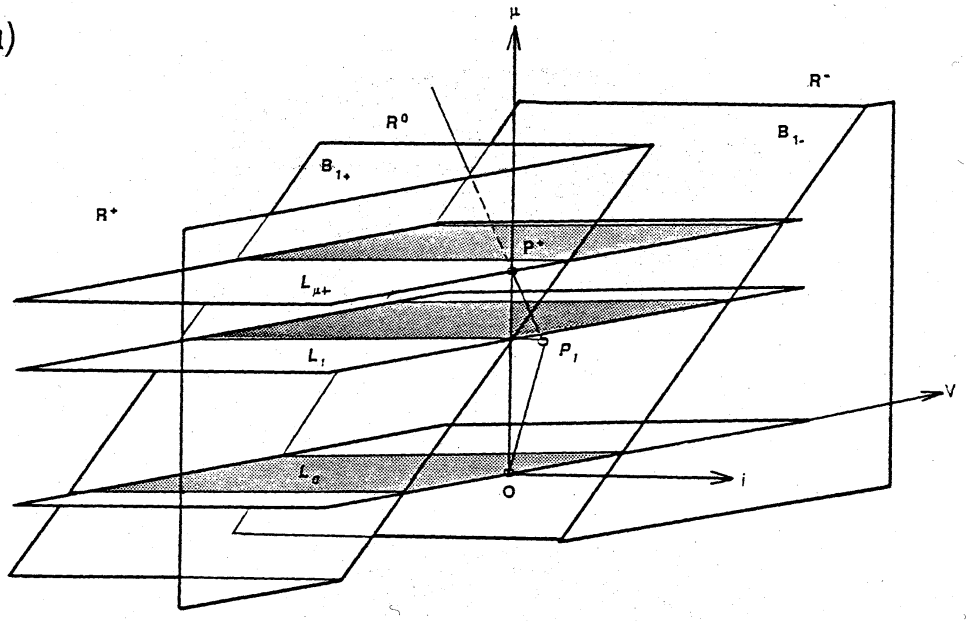

(b)

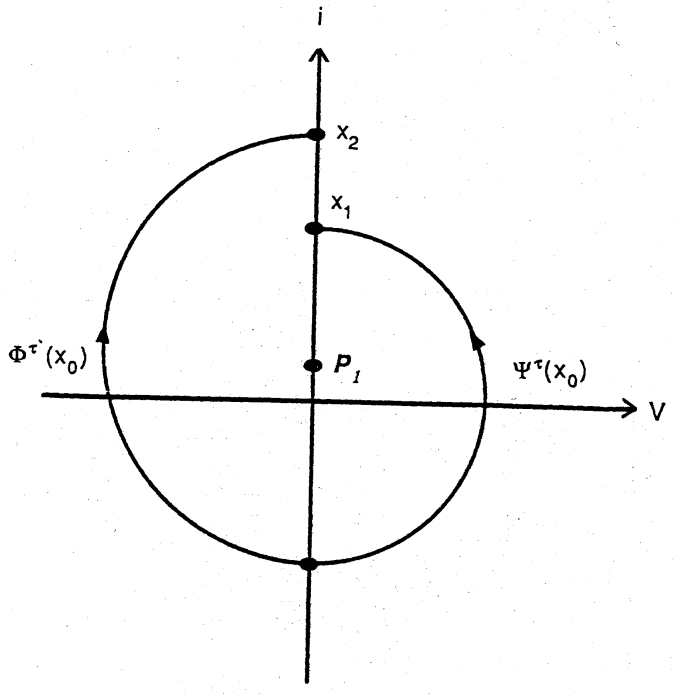

Figure 6

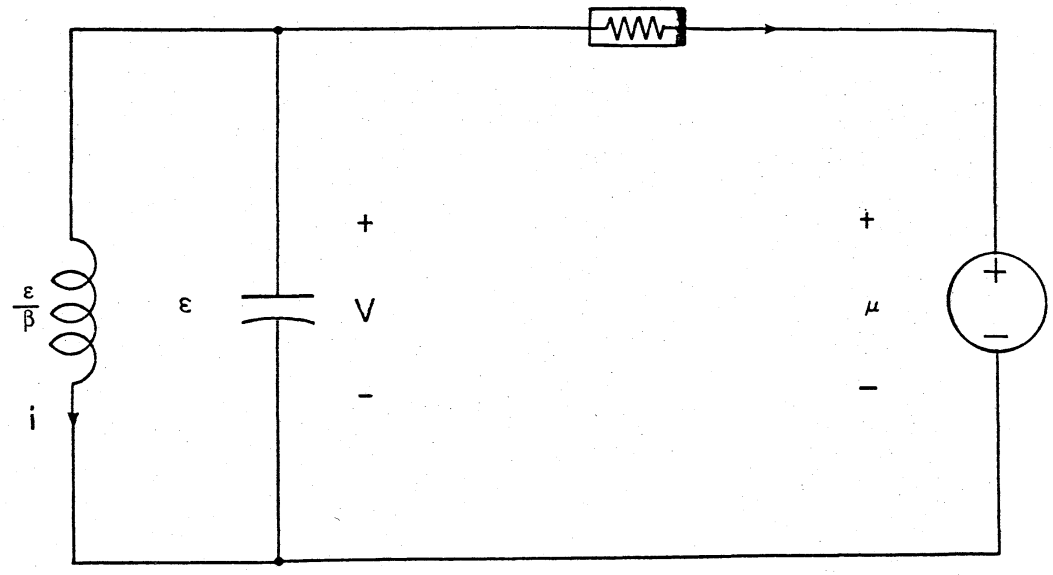

Figure 7

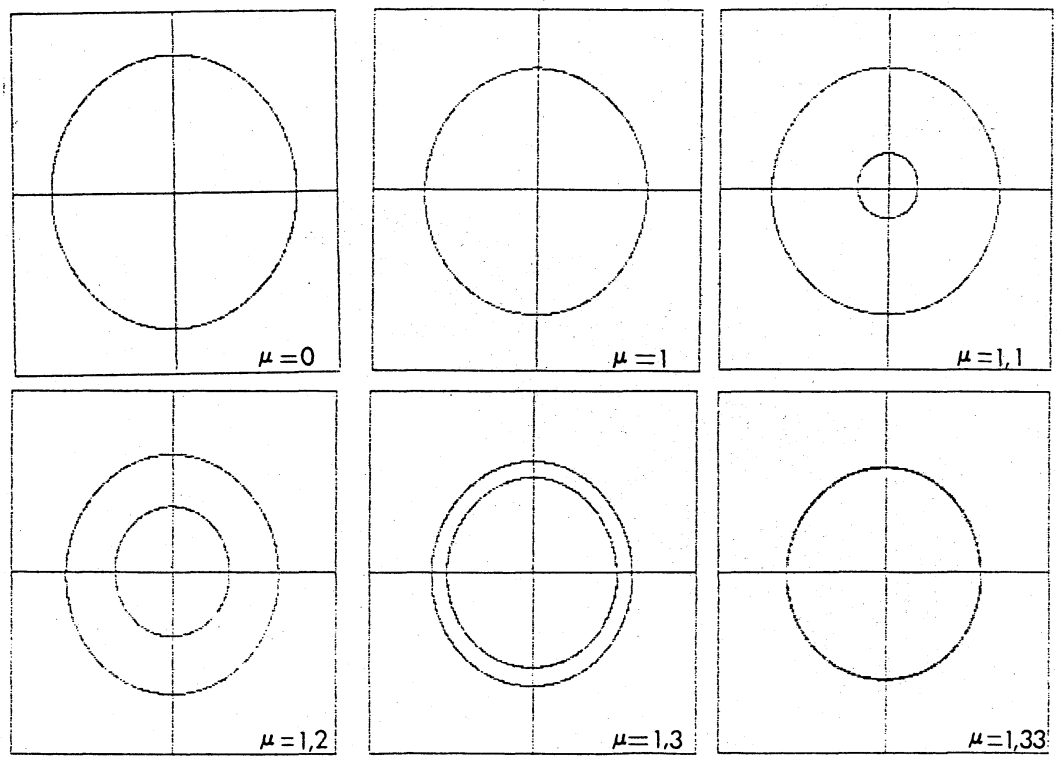

Figure 8

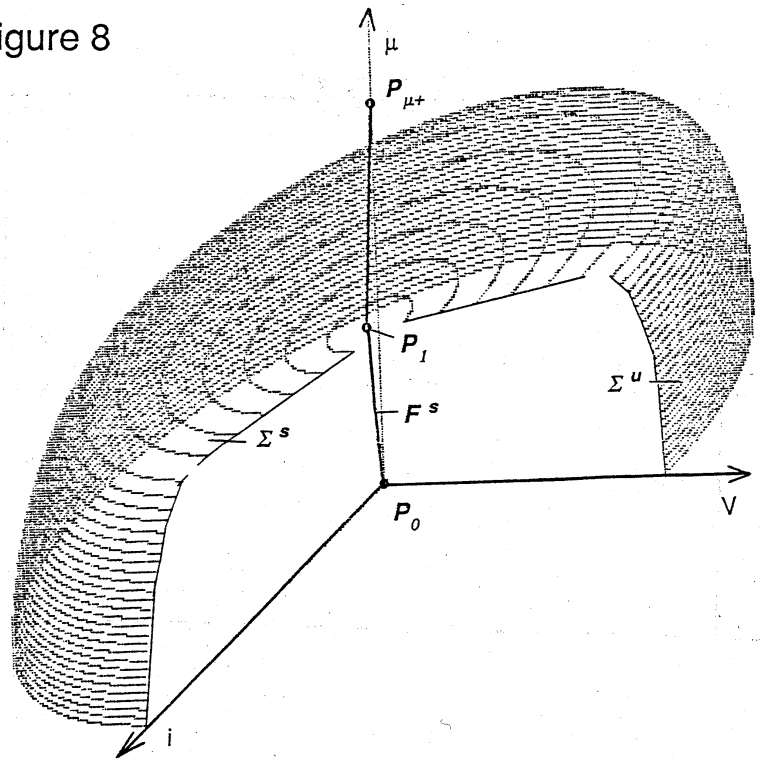

Figure 9

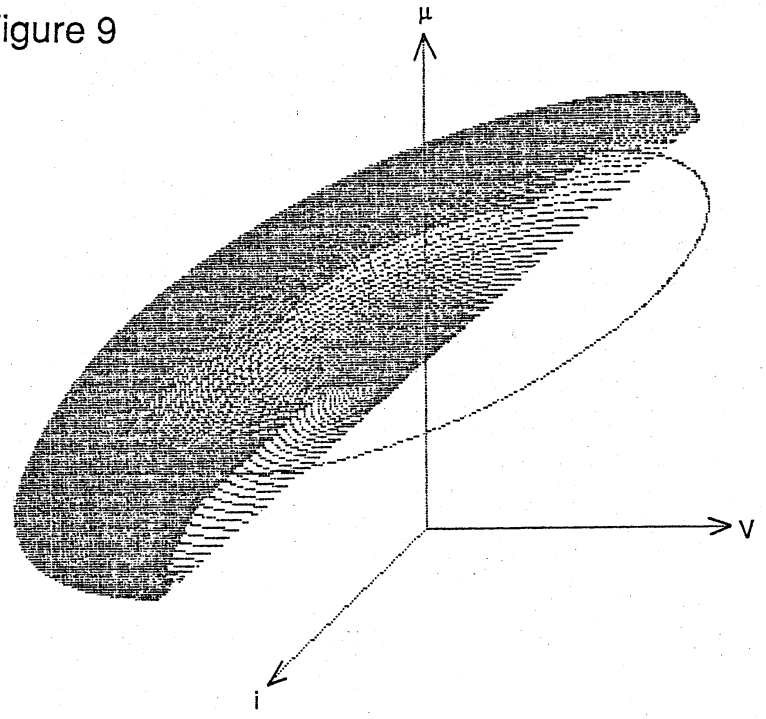

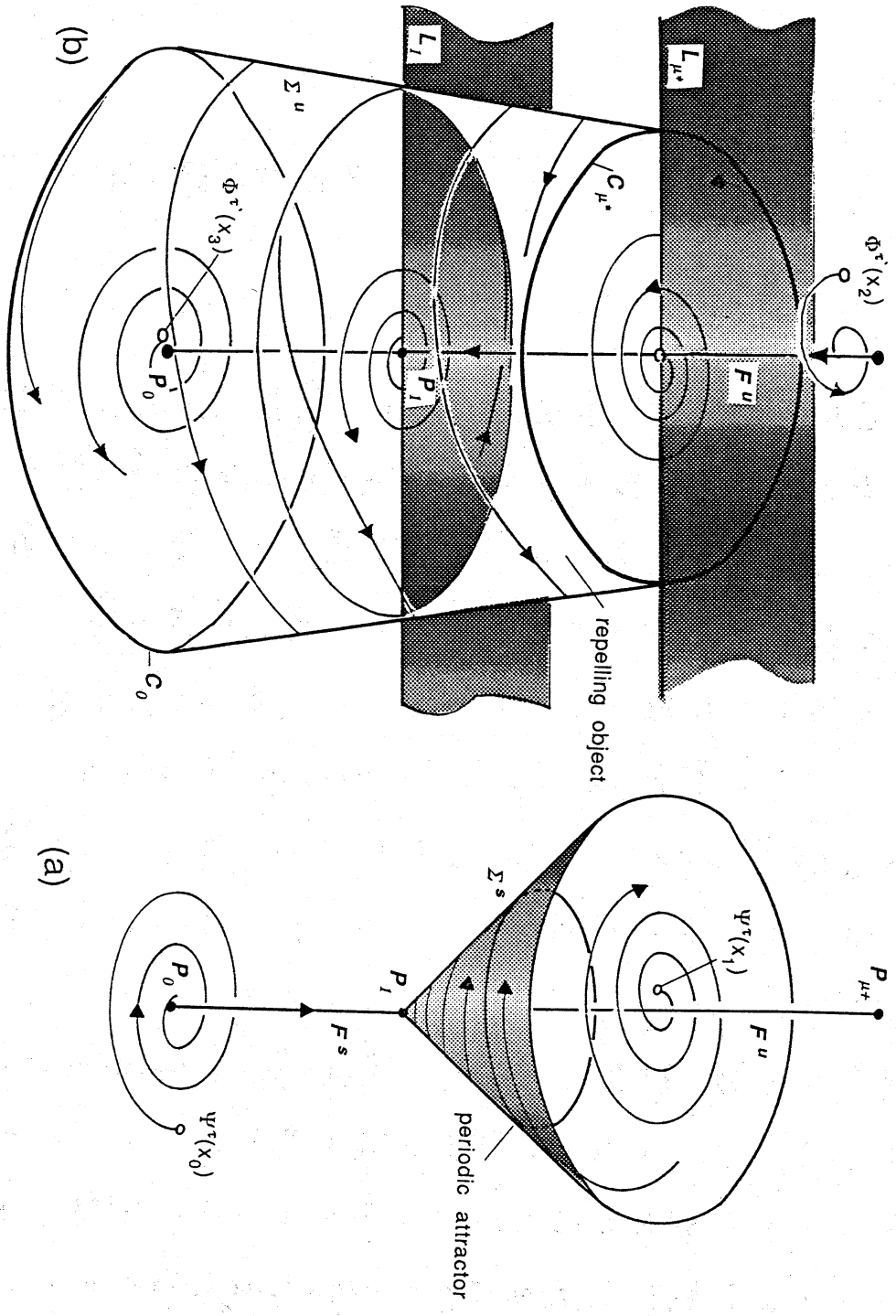
(a)
(b)
$P_{\mu+}$
F^u
$\Psi_\tau(x_1)$
Σ^s
P_1
F^s
P_0
$\Psi_\tau(x_0)$
periodic attractor
$L_{\mu+}$
L_1
$C_{\mu+}$
$\Phi_\tau(x_2)$
repelling object
Σ^u
$\Phi_\tau(x_3)$
P_1'
P_0'
C_0

Figure 10